Published in final edited form as:
J Cardiovasc Pharmacol. 2009 July ; 54(1): 47–56. doi:10.1097/FJC.0b013e3181ab371d.

Mechanism of Diastolic Stiffening of the Failing Myocardium and Its Prevention by Angiotensin Receptor and Calcium Channel Blockers

Xian Wu Cheng, MD, PhD[*,†], **Kenji Okumura, MD, PhD**[*], **Masafumi Kuzuya, MD, PhD**[‡], **Zhehu Jin, MD, PhD**[†,‡], **Kohzo Nagata, MD, PhD**[§], **Koji Obata, PhD**[¶], **Aiko Inoue, MS**[‡], **Akihiro Hirashiki, MD, PhD**[*], **Kyosuke Takeshita, MD, PhD**[*], **Kazumasa Unno, MD**[*], **Ken Harada, MD**[*], **Guo-Ping Shi, DSc**[||], **Mitsuhiro Yokota, MD, PhD**[**], and **Toyoaki Murohara, MD, PhD**[*]

[*] Department of Cardiology, Nagoya University Graduate School of Medicine, Nagoya, Japan

[†] Department of Cardiology, Yanbian University Hospital, Yanji, China

[‡] Department of Geriatrics, Nagoya University Graduate School of Medicine, Nagoya, Japan

[§] Department of Medical Technology, Nagoya University School of Health Sciences, Nagoya, Japan

[¶] Department of Pharmacology, Aichi Gakuin University School of Dentistry, Nagoya, Japan

[||] Department of Cardiovascular Medicine, Brigham and Women's Hospital, Harvard Medical School, Boston, MA

[**] Department of Genome Science, Aichi Gakuin University School of Dentistry, Nagoya, Japan

Abstract

Objective—To investigate the mechanism responsible for the increased cardiac stiffness associated with hypertensive heart failure in Dahl salt-sensitive (DS) rats and the effects of treatment with the combination of a calcium channel blocker [azelnidipine (AZE)] and angiotensin II type 1 receptor blocker [olmesartan (OLM)].

Methods—DS rats fed a high-salt diet from 7 weeks of age were treated (or not) from 12 to 19 weeks of age with the vasodilator hydralazine, OLM plus AZE, or the reduced nicotinamide adenine dinucleotide phosphate (NADPH) oxidase inhibitor apocynin. Rats fed a low-salt diet served as controls.

Results—Treatment with OLM plus AZE attenuated changes in the expression of collagen isoforms and a decrease in the ratio of elastin to collagen in the left ventricle and prevented the increase in myocardial stiffness and diastolic dysfunction in DS rats in a manner independent of the hypotensive effect of these drugs. Such treatment also inhibited the expression and activation of elastolytic proteases (including cathepsins S and K and metalloproteinases-2, -9, and -12), NADPH oxidase–dependent superoxide production, and inflammatory changes in the failing myocardium. All these effects were mimicked by treatment with apocynin.

Conclusions—The changes in collagen isoform expression and the decrease in the elastin to collagen ratio in the failing myocardium likely account for the increase in diastolic stiffness in this model of hypertensive heart failure. Administration of angiotensin receptor and calcium channel

Reprints: Xian Wu Cheng, MD, PhD, Department of Cardiology, Nagoya University School of Medicine, 65 Tsuruma-cho, Showa-ku, Nagoya 466-8550, Japan (xianwu@med.nagoya-u.ac.jp).

The authors report no conflicts of interest.

blockers prevented these changes in a manner independent of the hypotensive effect of these drugs by inhibiting the increase in elastolytic activity induced by activation of NADPH oxidase.

Keywords

cardiac stiffness; heart failure; collagen; elastin; oxidative stress; elastase

INTRODUCTION

Increased stiffness of the left ventricle (LV) during diastole is the earliest manifestation of hypertension-induced LV dysfunction and is often the main functional deficit of the heart associated with hypertension, given that many hypertensive patients who develop heart failure (HF) have a normal LV ejection fraction.[1,2] This increased LV stiffness is associated with marked changes in the extracellular matrix (ECM). Experimental and clinical studies have thus shown that hypertensive heart disease is accompanied by increased collagen expression, collagen density, and fibrillar collagen content and by altered fibrillar collagen geometry.[2–4] However, the specific molecular and biochemical mechanisms that underlie this ECM remodeling and the increase in LV stiffness in animals or patients with hypertensive heart disease have remained unclear. Two of the major determinants of ECM homeostasis are the rate and extent of ECM degradation. ECM degradation is mediated by cardiac cell–derived proteases such as matrix metalloproteinases (MMPs) and cysteine proteases.[1,3–5] Extensive evidence supports a role for MMPs in cardiac ECM remodeling,[1,5] and cathepsins, which are lysosomal cysteine proteases, show pronounced elastolytic and collagenolytic activities both in vitro and in vivo and are overexpressed in the failing myocardium of animals or patients with hypertension and dilated cardiomyopathy.[3,6–8] However, limited information has been available on cathepsin activation and its potential function in cardiac stiffening and ECM metabolism.

Both calcium channel blockers (CCBs) and angiotensin II type 1 receptor (AT_1R) blockers (ARBs) attenuate both cardiac dysfunction and ECM remodeling associated with HF in animal models.[2,9] Treatment of hypertensive patients with the combination of a CCB and an ARB has been shown to have a renoprotective effect and to be cost effective.[10] It has been reported that the combination of an ARB and a CCB has also shown to be a useful therapeutic strategy for the prevention of hypertensive heart failure.[11] However, the precise mechanisms underlying the cardioprotection afforded by the combination of a CCB and an ARB in animals or patients with hypertensive HF remain largely unknown. Oxidative stress is a hallmark of chronic HF, and the progression of cardiac hypertrophy to LV dysfunction can be prevented by treatment with antioxidants in animal models.[12,13] The cardiac and vascular protection conferred by CCBs and ARBs has been suggested to be attributable to antioxidant activity.

Dahl salt-sensitive (DS) rats are studied as a model of salt-sensitive hypertension in humans.[2,14] We have now investigated the changes in collagen and elastin expression and content and the relation between diastolic LV stiffness and the ratio of elastin to collagen in the LV of DS rats during the development of hypertensive HF. We have also examined the pharmacological mechanisms underlying the cardioprotection afforded by the combination of the ARB olmesartan (OLM) and the CCB azelnidipine (AZE) independently of the antihypertensive effect of these drugs in DS rats. We thus also treated DS rats fed a high-salt diet with the vasodilator hydralazine (HYD) or with apocynin (APO), an inhibitor of reduced nicotinamide adenine dinucleotide phosphate (NADPH) oxidase.

METHODS

Animals and Experimental Protocol

Male inbred DS rats were obtained from Japan SLC (Hamamatsu, Japan) and were handled in accordance with the guidelines of Nagoya University Graduate School of Medicine and with the Guide for the Care and Use of Laboratory Animals (National Institutes of Health publication no. 85-23, revised 1996). Weaning rats were fed laboratory chow containing 0.3% NaCl until 7 weeks of age. DS rats fed an 8% NaCl diet after 7 weeks manifest compensated concentric LV hypertrophy secondary to hypertension at 12 weeks and a distinct stage of fatal LV failure with lung congestion at 19 weeks.[3] DS rats were therefore fed an 8% NaCl diet from 7 weeks of age and were randomized to an untreated (HF) group, an HYD treatment group (10 mg/kg of body weight per day in drinking water), an OLM + AZE treatment group (3 and 6 mg/kg per day, respectively, in chow), and an APO treatment group (0.5 mmol/kg per day in drinking water) from 12 to 19 weeks of age (n = 10 for each group). APO was obtained from EMD Biosciences, Inc (La Jolla, CA), and both OLM and AZE were kindly provided by Sankyo Pharmaceutical, Co (Tokyo, Japan). DS rats fed a 0.3% NaCl diet after 7 weeks of age remain normotensive, and such animals served as age-matched controls (control group, n = 10). At 19 weeks of age, rats were anesthetized by intraperitoneal injection of ketamine (50 mg/kg) and xylazine (10 mg/kg) and were subjected to hemodynamic and echocardiographic analyses. The heart was subsequently excised, and LV tissue was either assayed for superoxide production, stored at −80°C for molecular analyses, or fixed with paraformaldehyde for pathological analysis.

Echocardiographic and Hemodynamic Analyses

Systolic blood pressure was measured weekly in conscious animals by tail-cuff plethysmography (BP-98A; Softron, Tokyo, Japan). At 19 weeks of age, rats were subjected to transthoracic echocardiography as previously described.[3] Echocardiography was performed with an SONOS 7500 ultrasound system and an ultraband transducer of 5–12 MHz (Philips, Andover, MA). LV end-diastolic (LVDd) and end-systolic (LVDs) dimensions and the thickness of the inter-ventricular septum were measured. LV fractional shortening was calculated as 100% × (LVDd − LVDs)/LVDd. The peak negative myocardial velocity gradient (MVG) was derived from tissue Doppler imaging as a measurement of diastolic function. After echocardiography, a 2F micromanometer-tipped catheter (SPR-407; Millar Instruments, Houston, TX) that had been calibrated relative to atmospheric pressure was inserted through the right carotid artery into the LV. We evaluated the maximum first derivative of LV pressure (LV dP/dt_{max}) as an index of contractility, minimal rate of LV pressure change (LV dP/dt_{min}), and the pressure half-time ($T_{1/2}$) as an index of relaxation. Tracings of LV pressure and the electrocardiogram were digitized to determine the pressure half-time and LV end-diastolic pressure.

Quantitative Reverse Transcription–Polymerase Chain Reaction Analysis

Total RNAwas isolated from LV tissue with the use of an RNeasy Fibrous Tissue Mini Kit (Qiagen, Inc, Valencia, CA) and was subjected to reverse transcription. The resulting complementary DNA was subjected to quantitative real-time polymerase chain reaction analysis with primers specific for monocyte chemoattractant protein (MCP)-1, connective tissue growth factor (CTGF), or osteopontin and with the use of an ABI 7300 Real-Time PCR System (Applied Biosystems, Foster City, CA), as previously described.[15,16] The amount of each messenger RNA (mRNA) was normalized by the corresponding amount of glyceraldehyde-3-phosphate dehydrogenase (GAPDH) mRNA.

Immunoblot Analysis

Tissue homogenates (50 μg of protein) were fractionated by sodium dodecyl sulfate–polyacrylamide gel electrophoresis, and the separated proteins were transferred to a polyvinylidene difluoride membrane (Amersham Pharmacia Biotech, Little Chalfont, Buckinghamshire, United Kingdom). The membrane was probed with antibodies to cathepsin S or cathepsin K[7,17]; to cathepsin L (Sigma-Aldrich, St. Louis, MO); to MMP-12 (Epitomics, Inc., Burlingame, CA); or to type Iα collagen, type III collagen, or GAPDH (Santa Cruz Biotechnology, Santa Cruz, CA). Immune complexes were detected with the use of enhanced chemiluminescence reagents and were quantified by scanning densitometry (Bio-Rad, Hercules, CA). The amounts of target proteins were normalized by that of GAPDH.

Zymography

In vitro zymography was performed as previously described.[15] In situ zymography was performed with a kit (MMP In Situ Zymo-Film; Wako, Pure Chemical Industries, Ltd., Osaka Japan)[1] and in the absence or presence of the MMP inhibitor EDTA (1 μmol/L), the cathepsin inhibitor *trans*-epoxysuccinyl-L-leucylamido-(4-guanidino)butane (E64, 20 μmol/L), or the serine protease inhibitor phenylmethyl-sulfonyl fluoride (2 mmol/L).

Measurement of Collagen and Elastin

Elastin was quantified as previously described.[18] In brief, LV rings were defatted in acetone and dried, and proteins were extracted from the dried tissue by agitation in 0.3% sodium dodecyl sulfate for 12 hours. ECM proteins other than elastin (including collagen) were solubilized by three 15-minute extractions in 0.1 mol/L NaOH performed in a boiling water bath, and elastin was quantified on the basis of the dry weight of the residue. Collagen content was determined by measurement with the use of a colorimetric assay[19] of the amount of hydroxyproline in the NaOH supernatants after their evaporation and hydrolysis of the residue in 6 M HCl for 24 hours at 110°C.

Immunohistochemistry

LV tissue was fixed with ice-cold 4% paraformaldehyde for 16 to 24 hours, embedded in paraffin wax, and processed for immunohistochemistry as described.[3,16] In brief, transverse sections (3 μm) were cut with a cryostat and stained with a mouse monoclonal antibody that recognizes rat macrophages (1:100 dilution; Chemicon, Temecula, CA) or with rabbit polyclonal antibodies to mouse CTGF (Torrey Pines Biolabs, Houston, TX). As a negative control, primary antibodies were replaced with nonimmune immunoglobulin G.

Assay of Superoxide Production, Glutathione, and Angiotensin II

Superoxide (O_2^-) production by total homogenates of fresh LV tissue was measured with the use of a lucigenin-based enhanced chemiluminescence assay as described.[20] A low lucigenin concentration (5 μmol/L) was used to minimize artifactual O_2^- production attributable to redox cycling. In brief, homogenate protein (1 mg) in 1 mL of lysis buffer [20 mmol/L Tris–HCl (pH 7.5), 150 mmol/L NaCl, 1 mmol/L EDTA, 1 mmol/L ethylene glycol tetraacetic acid, and 1% Triton X-100] was transferred to an assay tube, and NADPH and dark-adapted lucigenin were added to final concentrations of 100 and 5 μmol/L, respectively, immediately before the measurement of chemiluminescence. All assays were performed in triplicate. The chemiluminescence signal was sampled every minute for 12 minutes with a tube luminometer (20/20; Turner Biosystems, Sunnyvale, CA), and the respective background counts were subtracted from the experimental values.

The amount of total glutathione [reduced (GSH) plus oxidized (GSSG)] in LV tissue was determined by the recycling assay based on glutathione reductase and 5,5′-dithiobis-(2-

nitrobenzoic acid) as described.[21] Dihydroethidium staining for the production of superoxide was also performed as described.[22] In brief, myocardial sections (5 μm) cut with a cryostat were treated with acetone for 10 minutes and then incubated for 30 minutes at 37°C with 5 μmol/L dihydroethidium in phosphate-buffered saline. The sections were then examined with a laser scanning confocal microscope equipped with WinROOF version 5.0 image processing software (Mitani, Tokyo, Japan). The amount of angiotensin II in LV homogenates prepared in an ice-cold solution containing 25 mmol/L EDTA, 0.44 mmol/L 1,20-orthophenanthroline monohydrate, 1 mmol/L sodium parachloromercuribenzoate, and 3 μmol/L rat renin inhibitor acetyl-His-Pro-Phe-Val-Statine-Leu-Phe (WFML) was measured by radioimmunoassay and was normalized by LV weight.

Assay of Elastolytic Activity

Elastolytic activity in the myocardium was assayed as previously described.[3] Total LV homogenates (200 μg of protein) were incubated with fluorescein-conjugated DQ elastin (Molecular Probes, Eugene, OR) for 24 hours at 37°C, after which fluorescence was measured with a Fluoroskan Ascent CF instrument (Labsystems, Helsinki, Finland) at excitation and emission wavelengths of 485 and 530 nm, respectively. Data are presented as relative units after adjustment for background levels.

Statistical Analysis

Data were considered to be normally distributed and are presented as means ± SEM unless indicated otherwise. Differences were analyzed by Student *t* test or by 1-way analysis of variance followed by Scheffe multiple comparison test. A P value of <0.05 was considered statistically significant.

RESULTS

Hemodynamics and LV Structural and Functional Characteristics

At 19 weeks of age, neither heart rate nor body weight differed significantly among the 5 groups of DS rats (Table 1). Systolic blood pressure was higher in the HF group than in the control group at 8 weeks of age and thereafter (Fig. 1), whereas it was reduced in the HYD group and the OLM + AZE group at 13 weeks of age and thereafter compared with that in the HF group. There was no significant difference in systolic blood pressure between the HYD and OLM + AZE groups at 19 weeks of age ($P > 0.05$). The ratio of LV weight to body weight, an index of LV hypertrophy, was 59% greater in the HF group than in the control group at 19 weeks of age, and the increase in this parameter was attenuated by treatment with HYD, OLM + AZE, or APO (Table 1). Similarly, the ratio of lung wet weight to lung dry weight, an index of pulmonary congestion, was increased by 60% in HF rats compared with control rats, and this change was attenuated by treatment with HYD, OLM + AZE, or APO.

Both interventricular septum and LVDd were greater, whereas LV fractional shortening and LV dP/dt_{max} were smaller, in HF rats than in control rats. The changes in these parameters were inhibited by treatment with OLM + AZE and by that with HYD or APO (Table 1). The ratio of LV end-diastolic pressure and the $T_{1/2}$, an index of LV diastolic stiffness and relaxation, were also increased in the HF group, whereas the LV dP/dt_{min} was decreased in HF rats compared with control rats (Table 1). Treatment with OLM + AZE or with APO ameliorated all these changes in parameters of LV diastolic function, whereas HYD showed no benefit despite reducing systolic blood pressure by the same extent as did the combination therapy. Treatment with the combination of an ARB and a CCB thus inhibited LV remodeling, preserved LV systolic function, and attenuated LV diastolic dysfunction in a manner independent of its hypertensive action, and these effects were mimicked by treatment with APO.

Myocardial Collagen and Elastin Expression and Content

Quantitative analysis of immunoblots revealed that the amounts of types Iα and III collagen in LV tissue were increased in the HF group compared with the control group and that these changes were inhibited by all 3 drug treatments (Figs. 2A, B). The type III:Iα collagen ratio, which is thought to be negatively correlated with cardiac stiffness, tended to be smaller in the HF group than in the control group, but this difference was not statistically significant (Fig. 2C). This ratio was significantly decreased in the HYD and APO groups, but not in the OLM + AZE group, compared with the control group. A colorimetric assay confirmed that the total amount of hydroxyproline derived from collagen hydrolysis was increased in the HF group and that this increase was attenuated by treatment with HYD, OLM + AZE, or APO (Fig. 2D). In contrast, the ratio of elastin to collagen content was decreased in the HF group compared with the control group, and this change was attenuated by treatment with OLM + AZE or with APO but not by that with HYD (Fig. 2E). The elastin to collagen ratio was positively correlated with the peak negative MVG (Fig. 2F), which is itself negatively correlated with diastolic cardiac stiffness.

Myocardial MMP and Cathepsin Expression and Activity

Immunoblot analysis revealed that the amounts of the active forms of cathepsin S (28 kDa), cathepsin K (29 kDa), and MMP-12 (45 kDa) in the LV were increased in HF rats compared with control rats and that these increases were attenuated by treatment with OLM + AZE or APO (Figs. 3A–C). Consistent with these findings, elastolytic activity in the HF group was 4.4 times that in the control group, and this increase was attenuated in both OLM + AZE and APO groups (Table 1).

Gelatin zymography revealed major bands of 72 and 68 kDa for MMP-2 and 92 and 88 kDa for MMP-9 (Fig. 3D), corresponding to the latent and active forms, respectively, of these proteases,[15,23] in LV tissue. Quantitation of the data showed that the total gelatinolytic activity (pro plus active forms) of MMP-2 or MMP-9 was increased in the HF group relative to the control group and that these changes were suppressed by treatment with OLM + AZE or APO (Figs. 3E, F). The ratio of activated MMP-2 to total MMP-2, an index of net MMP-2 activation, was also increased in HF rats ($P < 0.05$) in a manner sensitive to treatment with OLM + AZE or APO (data not shown, $P < 0.05$). In situ zymography further confirmed that gelatinolytic activity was increased in HF rats (Fig. 3G); the activity was inhibited by EDTA and by E64 but not by phenylmethylsulfonyl fluoride, suggesting that it was attributable to MMPs and cysteine proteases rather than to serine proteases. HYD had no effect on the expression or activity of cathepsins or MMPs in the myocardium of DS rats fed a high-salt diet (Figs. 3A–F).

Myocardial Inflammation

Immunostaining revealed prominent macrophage infiltration in the LVof HF rats at 19 weeks of age (Figs. 4A, C). This infiltration was accompanied by increases in the abundance of mRNAs for MCP-1 and osteopontin (Figs. 4D, E). These inflammatory changes were attenuated by treatment with OLM + AZE or APO but not by that with HYD. The amounts of CTGF mRNA and protein were also increased in HF rats in a manner sensitive to treatment with OLM + AZE or APO but not to that with HYD (Figs. 4B, F).

Myocardial Oxidative Stress

Staining with dihydroethidium revealed that superoxide (O_2^-) production in myocardial tissue sections was increased in HF rats relative to that in control rats and that this increase was attenuated by treatment with OLM + AZE or APO but not by that with HYD (Fig. 5A). The NADPH oxidase–dependent production of O_2^- in LV tissue was also greater for HF rats than

for control rats, and this increase was attenuated by treatment with OLM + AZE or APO but by that with HYD (Fig. 5B). The generation of O_2^- in LV homogenates of HF rats was largely abolished by the flavoprotein inhibitor diphenyleneiodonium (data not shown), suggesting that NADPH oxidase was indeed the likely source of the superoxide. The glutathione redox ratio (GSH:GSSG) was decreased in LV tissue of HF rats compared with control rats, and this change was prevented by treatment with OLM + AZE or APO but not by that with HYD (Fig. 5C). Finally, the amount of angiotensin II in the LV was increased in HF rats relative to control rats in a manner sensitive to treatment with OLM + AZE but not to that with HYD or APO (Table 1).

DISCUSSION

We have made several important observations in the present study. First, failing myocardium of DS rats with hypertension is definitively characterized by an excessive diastolic LV stiffness associated with changes in the protein levels of collagen isoforms and decreases in the ratio of elastin protein to collagen protein. Second, NADPH oxidase is the responsible enzyme, and selective reduction of NADPH oxidase activity significantly reduced the activation and activity of elastolytic protease and local O_2^- generation in failing myocardium of DS rats. The APO-mediated antioxidative and anti-inflammatory effects are compatible with those in cardiac structural remodeling and diastolic dysfunction. Third, the administration of OLM + AZE to failing hearts in DS rats ameliorated LV remodeling and diastolic dysfunction concomitant with suppressed myocardial collagen accumulation, redressed the balance between elastin and collagen, decreased local O_2^- generation and inflammatory changes, and suppressed elastolytic protease activation and activity, whereas HYD showed no benefit despite similar decreases in blood pressure.

Collagen constitutes up to 85% of ECM in the heart, with the myocardial collagen network consisting predominantly of collagen types I and III.[24,25] Collagen type I confers rigidity, whereas collagen type III contributes to tissue elasticity. Collagen type I is thus thought to be a major determinant of myocardial stiffness,[24] and a decrease in the ratio of collagen type III to type I expression has been associated with increased myocardial stiffness.[4] However, previous studies have examined such changes in collagen isoform expression only at the mRNA level. We have now examined collagen expression by immunoblot analysis and determined collagen content by measurement of hydroxyproline derived from collagen hydrolysis. We found that the amounts of type Iα and type III collagen were significantly increased, whereas the type III to type Iα collagen ratio tended to be decreased, in HF rats. These findings demonstrated that the collagen type mRNA III to type I mRNA ratio may not be a good predictor of cardiac stiffness in this animal model of HF. A decrease in the elastin to collagen ratio has been proposed to be responsible for an increase in arterial stiffness in animals and humans.[18,26] We observed that the elastin to collagen ratio in the LV was decreased in HF rats and that this ratio was positively correlated with the peak negative MVG. Our findings demonstrated that the decrease in the elastin to collagen ratio underlies the increase in LV stiffness in DS rats with HF. The decrease in the elastin to collagen ratio associated with the development of HF was prevented by treatment with OLM + AZE or with APO but not by that with HYD.

Elastin degradation is thought to be mediated by MMPs and cathepsins.[6,27,28] Both MMP-2 and MMP-9 have previously been implicated in the development and progression of myocardial remodeling and in LV dilation.[1,5,29] We have now shown that treatment with OLM + AZE or APO inhibited the increases in cathepsin and MMP-12 expression, in the gelatinolytic activities of MMP-2 and MMP-9 and in total elastolytic activity associated with the development of HF in DS rats. MMP-9 and cathepsin S were previously shown to promote elastin disruption associated with atherosclerosis.[30,31] MMPs and cathepsins have also been

shown to be produced by resident cardiac cells and to manifest marked collagenolytic and elastolytic activities.[6,7,17] Our findings demonstrated that treatment with OLM + AZE prevents LV fibrosis and the decrease in the elastin to collagen ratio through inhibition of the expression and activation of elastolytic proteases. The levels of CTGF mRNA and protein were also increased in the failing myocardium of DS rats, and these effects were ameliorated by treatment with OLM + AZE or APO. Upregulation of *CTGF* gene expression has previously been associated with HF,[16] and NADPH oxidase–dependent production of reactive oxygen species was shown to be responsible for an increase in *CTGF* gene expression in the aorta of diabetic mice.[32] *CTGF* gene expression is also rapidly increased on exposure of cardiac myocytes to prohypertrophic stimuli,[33] consistent with the notion that upregulation of this growth factor contributes to cardiac hypertrophy and fibrosis. The observed inhibition of *CTGF* gene expression by OLM + AZE in the myocardium of hypertensive DS rats, likely resulting from a reduction in the extent of NADPH oxidase–dependent superoxide production, may thus have contributed, at least in part, to the attenuation of cardiac ECM remodeling and HF.

A phagocyte-type NADPH oxidase is thought to serve as a prominent source of reactive oxygen species in the myocardium.[22] Superoxide generation by NADPH oxidase has also been shown to result in the activation of several proteases and to contribute to cardiac remodeling.[12,34] Our results now indicate that NADPH oxidase is a major source of O_2^- in the failing myocardium of DS rats and that selective inhibition of NADPH oxidase activity reduces not only the level of O_2^- but also the activity of elastolytic proteases (MMPs and cathepsins). These findings, together with previous observations suggesting that both CCBs and ARBs exert antioxidant activity[35,36] and that blockade of Ca^{2+} channels or angiotensin II action reduces the extent of proteolysis associated with various cardiovascular injuries,[30] suggest that the inhibition of proteolysis resulting from the antioxidant activity of OLM + AZE is largely responsible for the cardioprotective effects of this drug combination. NADPH oxidase–derived O_2^- has been implicated as an important mediator of angiotensin II signaling.[37] Angiotensin II induces oxidative stress through the AT_1R-mediated activation of NADPH oxidase.[13] We found that the concentration of angiotensin II was increased in the myocardium of HF rats in a manner sensitive to treatment with OLM + AZE. The beneficial effects of OLM + AZE are thus likely also attributable to a reduction in AT_1R-mediated myocardial oxidative stress associated with a reduction in the local concentration of angiotensin II.

Oxidative stress induces the expression of redox-sensitive genes for chemoattractant proteins such as MCP-1 and for cell adhesion molecules. The superoxide anion is thought to function as a signaling molecule that mediates an increase in the activity of the transcription factor nuclear factor κB, which in turn contributes to the upregulation of such proinflammatory genes.[38] Macrophage infiltration into the failing myocardium of DS rats was accompanied by upregulation of the expression of *MCP-1* and osteopontin genes in the present study. The observation that these effects were abrogated by treatment with APO suggests that the myocardial inflammatory response is induced by activation of NADPH oxidase and contributes to the cardiovascular injury and fibrosis apparent in this model of HF. Macrophages play a key role in the production and release of MMPs and cathepsins associated with atherosclerosis.[39] Histochemical staining for macrophages in the failing myocardium of DS rats was previously shown to colocalize with that for MMP-2 and MMP-9, but the staining for MMP-2 and MMP-9 was not necessarily colocalized with that for macrophages.[1] We previously showed that the abundance of cathepsin S and cathepsin K mRNAs and proteins was markedly increased throughout the myocardium of DS rats with HF, with staining apparent in both cardiomyocytes and smooth muscle cells.[3] These findings demonstrated that macrophages contribute to the production and secretion of MMPs and cathepsins but are not the only cell type to express these proteases. Restraint of the inflammatory process by treatment with OLM + AZE thus likely contributes to the reduction in MMP and cathepsin expression induced by this drug combination.

Plasma renin, angiotensin II, and aldosterone levels were reportedly reduced in hypertensive DS rats.[16,40] It has recently been reported that local angiotensin-converting enzyme and AT_1R mRNA levels were upregulated in the LVof humans and rats with HF.[16,40] These observations suggested that the local angiotensin system in the LV myocardium may thus be activated in this low-renin hypertensive rat model. This notion is supported by our current observation that local tissue angiotensin II level in the LV myocardium was higher in DS HF rats than in control rats, and this change was reduced by treatment with OLM + AZE. Additionally, previous studies have shown that the primary dysfunction is in the kidney in DS rat model, and the development of LV failure parallels the deterioration of renal function.[41–44] Furthermore, it was demonstrated that impairment of renal dysfunction (specifically salt metabolism) plays an important role in the pathogenesis of HF.[44,45] These findings suggested that the beneficial effects of combination with OLM and AZE might be also attributable to improvement of salt/water balance or/and renal function in this model. Further investigations into these issues are required.

In summary, our findings suggest that changes in the expression of collagen isoforms and a decrease in the ratio of elastin to collagen may account for the increase in stiffness of the failing myocardium in DS rats. Furthermore, increased oxidative stress appears to be a driver for the activation of the elastolytic proteases. The observed cardioprotective effects of the combination of OLM (an ARB) and AZE (a CCB) are likely attributable, at least in part, to prevention of these changes in collagen isoform expression and the elastin to collagen ratio in the failing myocardium as a result of the inhibition of NADPH oxidase–dependent superoxide generation and inflammation.

Acknowledgments

Supported in part by grants from the Ministry of Education, Culture, Sports, Science, and Technology of Japan (nos. 17590719 and 19590812 to X.W.C.) and from the Japan Heart Foundation (no. 26-7508 to X.W.C.); by a Japan Heart Foundation/Novartis Research Award on Molecular and Cellular Cardiology (no. 26-7523 to X.W.C); and by a grant from the Takeda Science Foundation (no. 26-7527 to X.W.C).

References

1. Sakata Y, Yamamoto K, Mano T, et al. Activation of matrix metalloproteinases precedes left ventricular remodeling in hypertensive heart failure rats: its inhibition as a primary effect of angiotensin-converting enzyme inhibitor. Circulation 2004;109:2143–2149. [PubMed: 15051632]
2. Kim S, Yoshiyama M, Izumi Y, et al. Effects of combination of ACE inhibitor and angiotensin receptor blocker on cardiac remodeling, cardiac function, and survival in rat heart failure. Circulation 2001;103:148–154. [PubMed: 11136700]
3. Cheng XW, Obata K, Kuzuya M, et al. Elastolytic cathepsin induction/activation system exists in myocardium and is upregulated in hypertensive heart failure. Hypertension 2006;48:979–987. [PubMed: 16982960]
4. Saka M, Obata K, Ichihara S, et al. Pitavastatin improves cardiac function and survival in association with suppression of the myocardial endothelin system in a rat model of hypertensive heart failure. J Cardiovasc Pharmacol 2006;47:770–779. [PubMed: 16810078]
5. Duhaney TA, Cui L, Rude MK, et al. Peroxisome proliferator-activated receptor alpha-independent actions of fenofibrate exacerbates left ventricular dilation and fibrosis in chronic pressure overload. Hypertension 2007;49:1084–1094. [PubMed: 17353509]
6. Cheng XW, Kuzuya M, Nakamura K, et al. Localization of cysteine protease, cathepsin S, to the surface of vascular smooth muscle cells by association with integrin αvβ3. Am J Pathol 2006;168:685–694. [PubMed: 16436681]
7. Shi GP, Sukhova GK, Kuzuya M, et al. Deficiency of the cysteine protease cathepsin S impairs microvessel growth. Circ Res 2003;92:493–500. [PubMed: 12600886]

8. Stypmann J, Glaser K, Roth W, et al. Dilated cardiomyopathy in mice deficient for the lysosomal cysteine peptidase cathepsin L. Proc Natl Acad Sci U S A 2002;99:6234–6239. [PubMed: 11972068]
9. Okuda N, Hayashi T, Mori, et al. Nifedipine enhances the cardioprotective effects of an angiotensin-II receptor blocker in an experimental animal model of heart failure. Hypertens Res 2005;28:431–438. [PubMed: 16156507]
10. Saito I, Kobayashi M, Matsushita Y, et al. Cost-utility analysis of antihypertensive combination therapy in Japan by a Monte Carlo simulation model. Hypertens Res 2008;31:1373–1383. [PubMed: 18957808]
11. Kim-Mitsuyama S, Izumi Y, Yoshhida K, et al. Additive beneficial of the combination of a calcium channel blocker and angiotensin blocker on a hypertensive rat-heart failure model. Hypertens Res 2004;27:771–779. [PubMed: 15785013]
12. Doerries C, Grote K, Hilfiker-Kleiner D, et al. Critical role of the NAD(P)H oxidase subunit p47phox for left ventricular remodeling/dysfunction and survival after myocardial infarction. Circ Res 2007;100:894–903. [PubMed: 17332431]
13. Gao L, Wang W, Li YL, et al. Sympathoexcitation by central ANG II: roles for AT1 receptor upregulation and NAD(P)H oxidase in RVLM. Am J Physiol Heart Circ Physiol 2005;288:H2271–H2279. [PubMed: 15637113]
14. Yoshida J, Yamamoto K, Mano T, et al. AT1 receptor blocker added to ACE inhibitor provides benefits at advanced stage of hypertensive diastolic heart failure. Hypertension 2004;43:686–691. [PubMed: 14757777]
15. Cheng XW, Kuzuya M, Nakamura K, et al. Mechanisms underlying the impairment of ischemia-induced neovascularization in matrix metalloproteinase 2-deficient mice. Circ Res 2007;100:904–913. [PubMed: 17322177]
16. Nagata K, Obata K, Xu J, et al. Mineralocorticoid receptor antagonism attenuates cardiac hypertrophy and failure in low-aldosterone hypertensive rats. Hypertension 2006;47:656–664. [PubMed: 16505208]
17. Cheng XW, Kuzuya M, Sasaki T, et al. Increased expression of elastolytic cysteine proteases, cathepsins S and K, in the neointima of balloon-injured rat carotid arteries. Am J Pathol 2004;164:243–251. [PubMed: 14695337]
18. Qiu H, Depre C, Ghosh K, et al. Mechanism of gender-specific differences in aortic stiffness with aging in nonhuman primates. Circulation 2007;116:669–676. [PubMed: 17664374]
19. Behmoaras J, Osborne-Pellegrin M, Gauguier D, et al. Characteristics of the aortic elastic network and related phenotypes in seven inbred rat strains. Am J Physiol Heart Circ Physiol 2005;288:H769–H777. [PubMed: 15471977]
20. Maack C, Kartes T, Kilter H, et al. Oxygen free radical release in human failing myocardium is associated with increased activity of rac1-GTPase and represents a target for statin treatment. Circulation 2003;108:1567–1574. [PubMed: 12963641]
21. Tietze F. Enzymic method for quantitative determination of nanogram amounts of total and oxidized glutathione: applications to mammalian blood and other tissues. Anal Biochem 1969;27:502–522. [PubMed: 4388022]
22. Tao L, Gao E, Jiao X, et al. Adiponectin cardioprotection after myocardial ischemia/reperfusion involves the reduction of oxidative/nitrative stress. Circulation 2007;115:1408–1416. [PubMed: 17339545]
23. Cheng XW, Kuzuya M, Nakamura K, et al. Mechanisms of the inhibitory effect of epigallocatechin-3-gallate on cultured human vascular smooth muscle cell invasion. Arterioscler Thromb Vasc Biol 2005;25:1864–1870. [PubMed: 16051878]
24. Heeneman S, Cleutjens JP, Faber BC, et al. The dynamic extracellular matrix: intervention strategies during heart failure and atherosclerosis. J Pathol 2003;200:516–525. [PubMed: 12845619]
25. Marijianowski MM, Teeling P, Mann J, et al. Dilated cardiomyopathy is associated with an increase in the type I/type III collagen ratio: a quantitative assessment. J Am Coll Cardiol 1995;25:1263–1272. [PubMed: 7722119]
26. Cattell MA, Anderson JC, Hasleton PS. Age-related changes in amounts and concentrations of collagen and elastin in normotensive human thoracic aorta. Clin Chim Acta 1996;245:73–84. [PubMed: 8646817]

27. Novinec M, Grass RN, Stark WJ, et al. Interaction between human cathepsins K, L, and S and elastins: mechanism of elastinolysis and inhibition by macromolecular inhibitors. J Biol Chem 2007;282:7893–7902. [PubMed: 17227755]
28. Senior RM, Griffin GL, Fliszar CJ, et al. Human 92- and 72-kilodalton type IV collagenases are elastases. J Biol Chem 1991;266:7870–7875. [PubMed: 1850424]
29. Lebrasseur NK, Duhaney TA, De Silva DS, et al. Effects of fenofibrate on cardiac remodeling in aldosterone-induced hypertension. Hypertension 2007;50:489–496. [PubMed: 17606858]
30. Suganuma E, Babaev VR, Motojima M, et al. Angiotensin inhibition decreases progression of advanced atherosclerosis and stabilizes established atherosclerotic plaques. J Am Soc Nephrol 2007;18:2311–2319. [PubMed: 17634441]
31. Abdul-Hussien H, Soekhoe RG, Weber E, et al. Collagen degradation in the abdominal aneurysm: a conspiracy of matrix metalloproteinase and cysteine collagenases. Am J Pathol 2007;170:809–817. [PubMed: 17322367]
32. San Martin A, Du P, Dikalova A, et al. Reactive oxygen species-selective regulation of aortic inflammatory gene expression in type 2 diabetes. Am J Physiol Heart Circ Physiol 2007;292:H2073–H2082. [PubMed: 17237245]
33. Kemp TJ, Aggeli IK, Sugden PH, et al. Phenylephrine and endothelin-1 upregulate connective tissue growth factor in neonatal rat cardiac myocytes. J Mol Cell Cardiol 2004;37:603–606. [PubMed: 15276029]
34. Grote K, Flach I, Luchtefeld M, et al. Mechanical stretch enhances mRNA expression and proenzyme release of matrix metalloproteinase-2 (MMP-2) via NAD(P)H oxidase-derived reactive oxygen species. Circ Res 2003;92:e80–e86. [PubMed: 12750313]
35. Jinno T, Iwai M, Li Z, et al. Calcium channel blocker azelnidipine enhances vascular protective effects of AT1 receptor blocker olmesartan. Hypertension 2004;43:263–269. [PubMed: 14707152]
36. Tsuda M, Iwai M, Li JM, et al. Inhibitory effects of AT1 receptor blocker, olmesartan, and estrogen on atherosclerosis via anti-oxidative stress. Hypertension 2005;45:545–551. [PubMed: 15723967]
37. Zimmerman MC, Lazartigues E, Lang JA, et al. Superoxide mediates the actions of angiotensin II in the central nervous system. Circ Res 2002;91:1038–1045. [PubMed: 12456490]
38. Collins T, Read MA, Neish AS, et al. Transcriptional regulation of endothelial cell adhesion molecules: NF-kappa B and cytokine-inducible enhancers. FASEB J 1995;9:899–909. [PubMed: 7542214]
39. Zalba G, Fortuno A, Orbe J, et al. Phagocytic NADPH oxidase-dependent superoxide production stimulates matrix metalloproteinase-9: implications for human atherosclerosis. Arterioscler Thromb Vasc Biol 2007;27:587–593. [PubMed: 17194891]
40. Cheng XW, Murohara T, Kuzuya M, et al. Superoxide-dependent activation of cysteine protease cathepsin system is associated with hypertensive myocardial remodeling and represents a target for angiotensin II type 1 receptor blocker therapy. Am J Pathol 2008;173:358–369. [PubMed: 18583318]
41. Yamazaki K, Katoh H, Yamamoto N, et al. Characterization of new inbred strains of Dlah-Iwai salt-sensitive and salt-resistant rats. Lab Anim Sci 1994;44:462–467. [PubMed: 7844954]
42. Miura N, Suzuki S, Hamada Y, et al. Salt water promotes hypertension in Dahl-S rats. Exp Anim 1999;48:289–292. [PubMed: 10591010]
43. Tsunooka N, Morita H. Effect of a chronic high-salt diet on whole-body and organ sodium contents of Dahl rats. J Hypertens 1997;15:851–856. [PubMed: 9280207]
44. Klotz S, Hay I, Zhang G, et al. Development of heart failure in chronic hypertensive Dahl rats: focus on heart failure with preserved ejection fraction. Hypertension 2006;47:901–911. [PubMed: 16585423]
45. Maurer MS, King DL, EI-Khoury Rumbarger L, et al. Left heart failure with a normal ejection fraction: identification of different pathophysiologic mechanisms. J Card Fail 2005;11:177–187. [PubMed: 15812744]

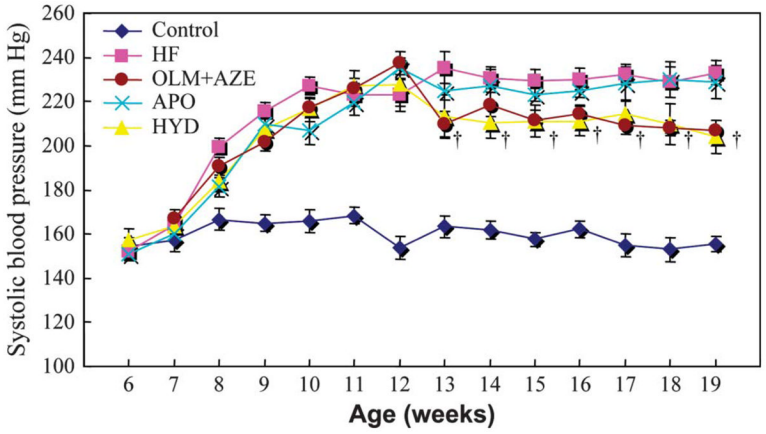

FIGURE 1.

Time course of systolic blood pressure in DS rats fed a high-salt diet and either left untreated (HF) or treated with HYD, with the combination of OLM and AZE (OLM + AZE) or with apocynin (APO). Results are also shown for age-matched DS rats fed a low-salt diet (control). Data are means ± SEM for 10 rats of each group. †$P < 0.05$ for HYD or OLM + AZE groups versus HF group.

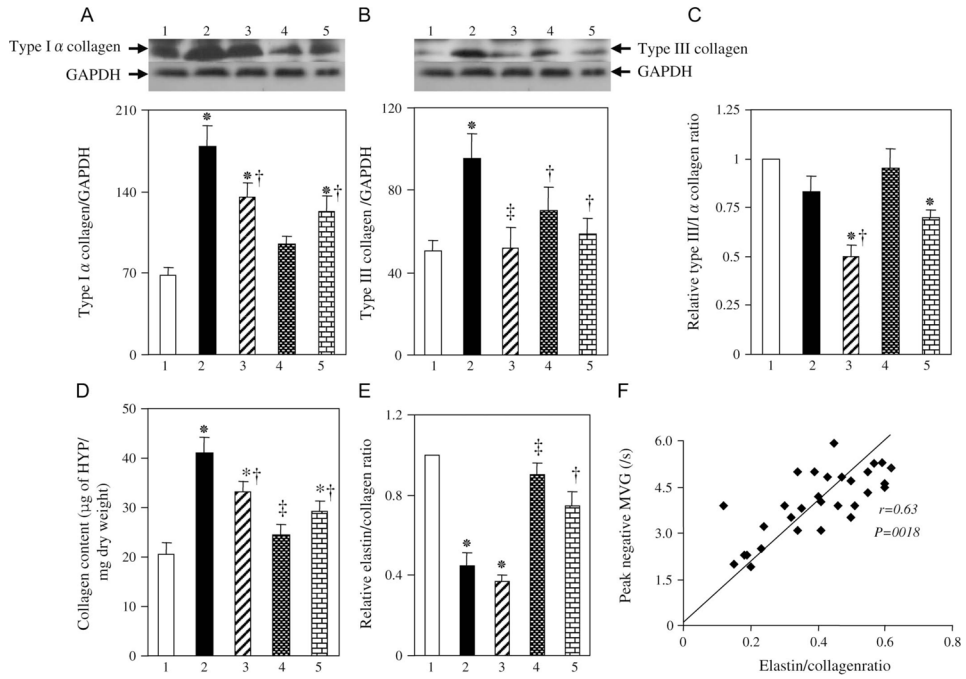

FIGURE 2.

Collagen and elastin expression in the LV of DS rats in the 5 experimental groups at 19 weeks of age. A, B, Immunoblot analysis of type Iα (A) and type III (B) collagen in the LV of rats of the control (1), HF (2), HYD (3), OLM + AZE (4), or APO (5) groups. Representative blots and densitometric analysis of the collagen to GAPDH ratio are shown in the upper and lower panels, respectively. C, Type III:Iα collagen ratio determined from immunoblots similar to those shown in (A) and (B). Data are expressed relative to the value for the control group. D, E, Collagen content (D) and the ratio of elastin to collagen contents (E) of the LV. Data in (D) are expressed as micrograms of hydroxyproline (HYP) per milligram of tissue dry weight, whereas those in (E) are expressed relative to the value for the control group. F, Relation of peak negative MVG to the elastin to collagen ratio for 6 rats of each group. Quantitative data in (A) to (E) are means ± SEM for 6 rats per group. *$P < 0.05$ versus control group; †$P < 0.05$, ‡$P < 0.01$ versus HF group.

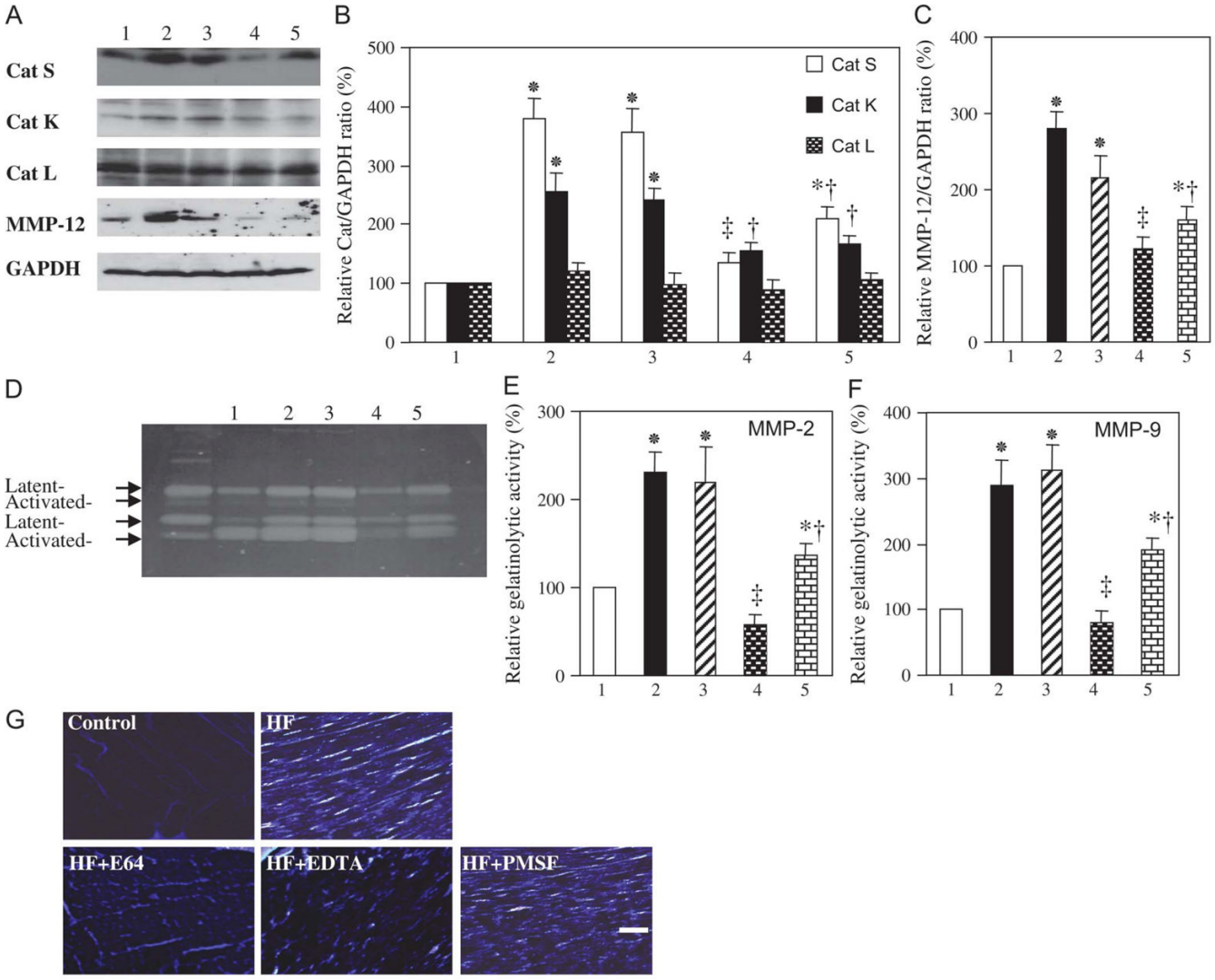

FIGURE 3.

Expression and activity of MMPs and cathepsins in the LV of DS rats in the 5 experimental groups at 19 weeks of age. A, Immunoblot analysis of cathepsins (Cats) S, K, and L and MMP-12 in the LV of rats of the control (1), HF (2), HYD (3), OLM + AZE (4), or APO (5) groups. B, C, Densitometric analysis of each cathepsin/GAPDH (B) or MMP-12:GAPDH (C) ratio determined from immunoblots similar to those shown in (A). Data are expressed as a percentage of the corresponding value for the control group and are means ± SEM for 6 rats of each group. **P* < 0.05 versus control group; †*P* < 0.05, ‡*P* < 0.01 versus HF group. D, Gelatin zymography of LV tissue homogenates. The 72- and 68-kDa bands for MMP-2 and the 92- and 88-kDa bands for MMP-9 correspond to the latent and active forms, respectively, of each protease. E, F, Total gelatinolytic activities of MMP-2 (E) and MMP-9 (F) were determined from quantitation of the latent and active forms of each protease in gels similar to that shown in (D). Data are expressed as a percentage of the corresponding value for the control group and are means ± SEM for 5 rats of each group. (G) In situ zymography of gelatinolytic activity in the LV of rats from the control and HF groups. Tissue from the HF rat was also incubated in the presence of EDTA (1 μmol/L), E64 (20 μmol/L), or PMSF (2 mmol/L). Brightness in the light microscopic images represents endogenous gelatinase activity. Scale bar: 50 μm. PMSF, phenylmethylsulfonyl fluoride.

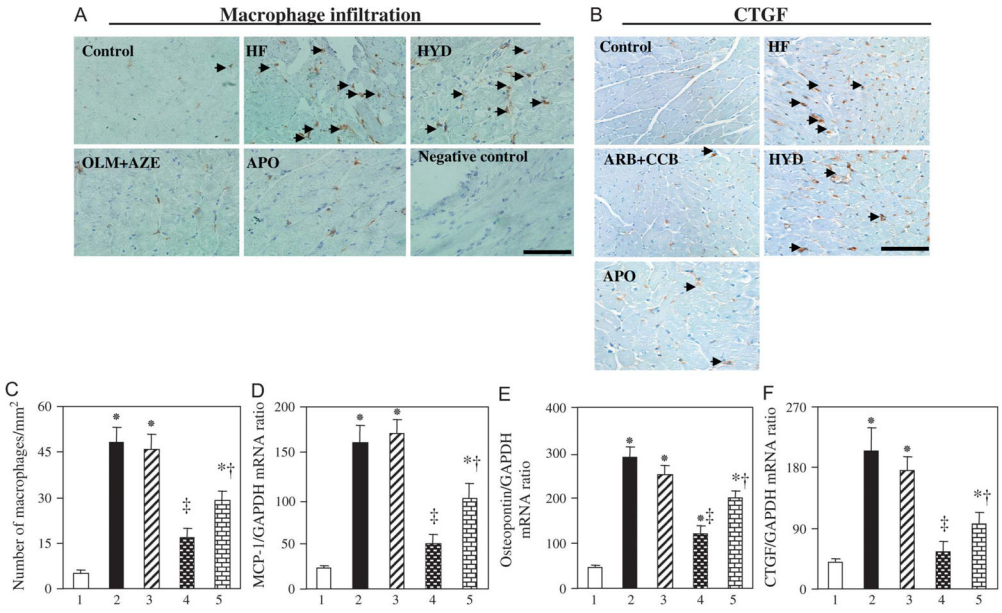

FIGURE 4.

Macrophage infiltration and expression of CTGF, MCP-1, and osteopontin in the LV of DS rats in the 5 experimental groups at 19 weeks of age. A, C, Representative immunohistochemical staining for macrophage infiltration in the LV is shown in (A). A section from an HF rat stained with nonimmune immunoglobulin G instead of primary antibodies is shown as a negative control. Arrowheads indicate macrophages. Scale bar: 100 μm. Quantitation of the number of infiltrated macrophages per square millimeter is shown in (C). Data are means ± SEM for 6 rats of each group. **P* < 0.05 versus control group; †*P* < 0.05, ‡*P* < 0.01 versus HF group. B, Representative immunohistochemical staining for CTGF in the LV. Arrowheads indicate immunoreactivity. Scale bar: 100 μm. D–F, Quantitative RT-PCR analysis of MCP-1, osteopontin, and CTGF mRNAs, respectively, in LV tissue of (1) control, (2) HF, (3) HYD, (4) OLM + AZE, and (5) APO groups. Data are means ± SEM for 6 rats of each group. RT-PCR, reverse transcription–polymerase chain reaction.

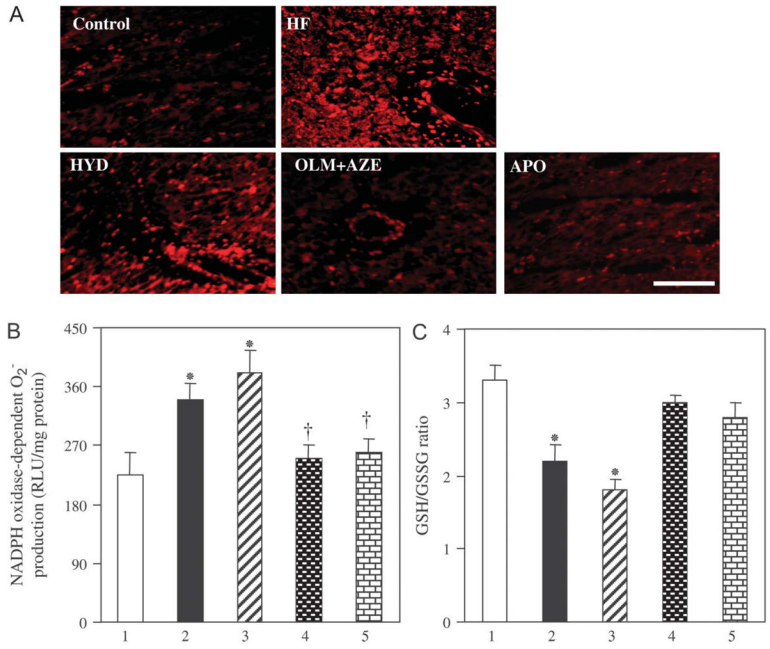

FIGURE 5.

Oxidative stress in the LV of DS rats in the 5 experimental groups at 19 weeks of age. A, Representative dihydroethidium staining for superoxide production in LV sections. Scar bar: 100 μm. B, NADPH oxidase–dependent O_2^- production in LV homogenates prepared from rats of the (1) control, (2) HF, (3) HYD, (4) OLM + AZE, and (5) APO groups. Data are expressed as relative light units (RLU) per milligram of protein and are means ± SEM for 6 rats of each group. *$P < 0.05$ versus control group; †$P < 0.05$ versus HF group. C, The GSH:GSSG ratio in LV tissue. Data are means ± SEM for 6 rats of each group.

J Cardiovasc Pharmacol. Author manuscript; available in PMC 2010 July 15.

TABLE 1

Hemodynamic, Echocardiographic, and Other Parameters for DS Rats in the 5 Experimental Groups at 19 Weeks of Age

Parameter	Control	HF	HYD	OLM + AZE	APO
Body weight (g)	417 ± 16	376 ± 24	406 ± 17	412 ± 19	401 ± 21
Heart rate (bpm)	416 ± 12	478 ± 23	501 ± 16	426 ± 18	450 ± 16
SBP (mm Hg)	151 ± 4	229 ± 3*	205 ± 208†	208 ± 5†	217 ± 6
LVW:BW (mg/g)	2.2 ± 0.1	3.5 ± 0.3*	2.7 ± 0.2†	2.4 ± 0.2‡	2.8 ± 0.3†
Lung weight (wet/dry)	4.2 ± 0.3	6.7 ± 0.5*	5.2 ± 0.4†	4.3 ± 0.3‡	4.9 ± 0.4†
IVST (mm)	1.4 ± 0.1	2.1 ± 0.1*	1.7 ± 0.1†	1.6 ± 0.1†	1.8 ± 0.1†
LVDd (mm)	7.1 ± 0.1	9.4 ± 0.4*	8.1 ± 0.2†	7.4 ± 0.2†	8.2 ± 0.3†
LVFS (%)	46 ± 1	34 ± 2*	43 ± 1†	48 ± 2†	41 ± 1†
dp/dt_{max} (mm Hg/s)	9284 ± 1124	7127 ± 927*	9467 ± 2034†	11,990 ± 1113‡	10,132 ± 2314†
dp/dt_{min} (mm Hg/s)	12,167 ± 1466	7796 ± 1019*	9039 ± 2405*	13,167 ± 917‡	10,800 ± 2014*†
$T_{1/2}$ (ms)	3.4 ± 0.1	5.5 ± 0.2*	4.9 ± 0.3*	3.7 ± 0.2‡	4.4 ± 0.2*†
LVEDP (mm Hg)	4.8 ± 0.5	16.5 ± 1.5*	14.5 ± 1.4*	6.9 ± 0.5‡	9.3 ± 1.5*†
Elastolytic activity	450 ± 56	1980 ± 134*	1810 ± 201*	750 ± 88†	1259 ± 109†
Ang II (pg/mg LVW)	155 ± 13	360 ± 43*	346 ± 51*	178 ± 45†	308 ± 65*

Elastolytic activity is expressed in fluorescence units. Data are means ± SEM for at least 6 animals of each group.

$^{*}P < 0.05$ versus control group;

$^{\dagger}P < 0.05$,

$^{\ddagger}P < 0.01$ versus HF group.

Ang II, angiotensin II; BW, body weight; IVST, interventricular septum; LVEDP, left ventricular end-diastolic pressure; LVFS, left ventricular fractional shortening; LVW, left ventricular weight; SBP, systolic blood pressure.